JOURNAL OF APPLIED ELECTROCHEMISTRY **28** (1998) 1313–1319

The 'memory effect' on nickel oxide electrodes: electrochemical and mechanical aspects*

G. DAVOLIO, E. SORAGNI

Department of Chemistry, University of Modena, 183, Via G. Campi, I 41100, Modena, Italy

Received 11 September 1997; revised 1 July 1998

Full discharge of nickel–cadmium batteries after sustained overcharge or repeated shallow discharge shows a voltage step generally known as the 'memory effect'. Nickel oxide electrode (NOE) gives a relevant contribution to the memory phenomenon, which has been related to the presence of the γ-phase. This phase, in fact, had been found by XRD analysis in a charged NOE showing such an effect. This work deals with the mechanical behaviour of NOEs cycled so as to produce the memory effect. During the cycling of asymmetric electrodes, a bending moment occurs during discharge: this is caused by the expansion of the active mass. The force, normal to the plane of the electrode, which equilibrates with the bending moment can be measured, thus giving an indication of the stresses suffered by the sintered supporting structure. Significant differences in both the electrochemical and mechanical behaviour after sustained overcharge and after shallow discharge have been observed. The different behaviours can be related to the unlike distribution of the γ-phase in the body of the electrode. It is suggested that the shallow cycling produces an accumulation of γ-phase at the contact with the current collector, whereas during sustained overcharge all the active mass is changed into γ-phase.

Keywords: *active mass expansion*, *internal stress*, *memory effect*, *nickel oxide electrode*

1. Introduction

Voltage–time discharge curves of sealed Ni–Cd batteries often show departures from the expected sigmoid shaped curve, depending on the cycling regime. A frequent feature is the appearance of a voltage step of about 0.1 V per cell: this means that the battery capacity is reduced at a fixed cut-off voltage, the residual capacity being delivered at a lower voltage.

The voltage step occurs in the complete discharge following a sustained overcharge [1] or several repeated partial discharges [2, 3]. In the latter case the voltage step appears at the same depth of the incomplete discharge. In the case of overcharge, the lower step is longer, the longer the overcharge has lasted. In both cases it is as if the battery had 'memorized' something of the previous history. A regular recharge (+10% overcharge) restores the usual shape of the voltage–time curve and the capacity. Initially the memory effect was attributed to physical changes in the negative cadmium electrode, caused by growth of the cadmium crystals during the overcharge: the decreased real surface of the electrode lowers the working voltage in discharge.

Another cause of the potential depression of the cadmium electrode was identified by Barnard *et al.* [4] as due to the formation of the Ni_5Cd_{21} alloy in overcharge. This alloy is formed only on sinter supported Cd plates, due to the highly intimate contact of the two fine-grained metals; no memory effect is reported on batteries with pocket or pasted Cd plates. Actually only the voltage steps in discharge following shallow cycles can be really seen as a 'memory effect', and properly Thomas [3] refers to the second phenomenon as to 'alloy formation'. In both cases the voltage step disappears after complete discharge.

Memory effects, with a voltage step, have also been observed in nickel–hydrogen and nickel–metal hydride cells after both overcharge and shallow discharge. These facts suggested that a significant contribution to the phenomenon originates from the nickel oxide electrode (NOE) [5, 6].

The aim of this work is to establish the conditions and factors influencing the phenomenon, in order to find additives and/or battery management methods that avoid failure and improve reliability in use. In this study, along with the classic charge–discharge cycling, mechanical tests on asymmetric electrodes have been carried out. This technique was used in previous NOE studies [7, 8].

Electrodes having different sinter thickness with respect to the current collector show an asymmetry which gives rise to bending, when an expansion of the active mass occurs. This is the particular case of the discharge of NOE. Figure 1 represents the longitudinal sections of an unstressed asymmetric electrode (NOE in the charged condition, Fig. 1(a), and of a stressed electrode (NOE discharged, Fig. 1(b)). The

*This paper is dedicated to the memory of Professor Giuseppe Bianchi.

0021-891X

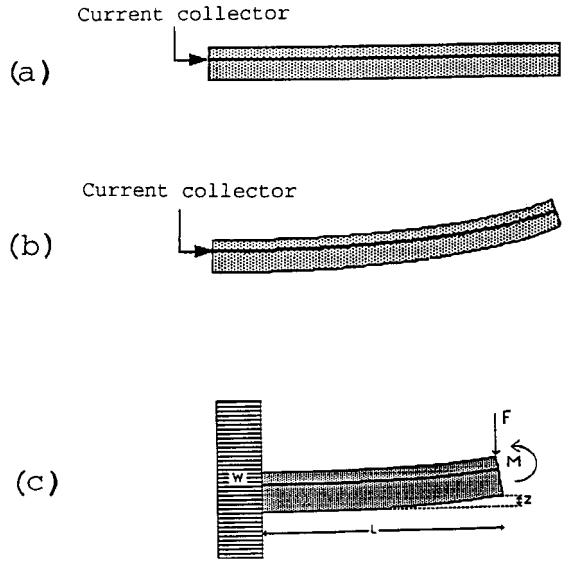

Fig. 1. Cross sections of an asymmetric NOE. (a) Charged (or uncycled), (b) discharged and (c) NOE as a cantilevered beam.

current collector acts as the neutral surface, owing to its higher stiffness with respect to the sinter, so the upper part of the electrode is highly stressed. If an asymmetric NOE is clamped at one end, during the discharge a bending moment, M, occurs, balanced by the stiffness of the supporting structure, with a displacement z at the free end. The bending moment is dependent upon the moment of the force, F, applied at the distance, L (to cancel the displacement z) and is given by $M = FL$ (Fig. 1(c)).

The bending moment is related to the elastic modulus, Y, which, in turn, depends on the volume fraction of the active mass, determined by the state of charge. A correlation between the volume changes and the bending moment may be derived by applying the principles of micromechanics of composite materials, such as sintered NOE. In the case of composites, with well defined structure, such as fibre reinforced plastics, it is possible to calculate the elastic modulus of the composite, as a function of the volume fractions and elastic moduli of the constituents [9].

The application of micromechanics theory to sintered NOE is difficult owing to the lack of knowledges about the real structure of the composite and the physical properties of the active mass. The elastic modulus of the active mass, for example, is not known, nor its dependence upon the state of charge.

In spite of these limits the theory may constitute an interesting qualitative approach to the problem of modelling the NOE and, in this respect, an aim of this work is to collect experimental data related to mechanical stresses produced by the memory-related cycling, and its effects on the electrode stability [10, 11].

2. Experimental details

Electrochemical and mechanical tests were performed on sintered nickel oxide electrodes, with the apparatus sketched in Fig. 2. One end of the electrode, E, was firmly fixed to the plexiglass cell. From the mechanics of deformable bodies, the theory of the cantilevered beam [12] gives the relation between the force applied, F, and the displacement, z. Referring to Fig. 1(c), Y being the Young's modulus, I the moment of inertia of the cross section ($I = bh^3/12$, for a beam of rectangular cross section of length b and height h), the displacement, z is given by

$$z = FL^3/3YI \tag{1}$$

With the value of z fixed and kept constant, in controlling the relative position of the balance the force F is a function of the sole variable Y and is therefore related to volume changes. It is thus a measure of the stresses on the structure. The force F was measured by means of an electronic balance, as the difference between the weight, W, hanging form the balance and the actual weight, W', or $F = W - W'$. In the cell we used $L = 2.5$ cm.

A Luggin capillary, not shown in the sketch, was connected to a mercuric oxide reference electrode. The counter electrode, CE, was a sintered cadmium plate.

Throughout a series of tests on one electrode the mechanical parameters of the apparatus were kept constant in order to compare the mechanical behaviour under different conditions. Change of the electrolyte, for example, was achieved by emptying and filling the cell without disturbing the cell.

The tests were conducted on three types of electrode: *type A* with chemical impregnation (Co content 2.9%); *type B* with electrochemical impregnation (Co content 4.3%); and *type C* with electrochemical impregnation (Co content 8.2%). All the test electrodes were manufactured with a nickel sinter as support, and a nickel net as current collector. The asymmetry was very high: for example, see the section of a type C electrode in Fig. 3.

Electrodes B and C were cut from ring-shaped nickel oxide plates for nickel–hydrogen cells, (ext. dia. 8.5 cm, int. dia. 3.5 cm). Electrode A was cut from a piece of a commercial plate. Electrode dimensions were 5 cm × 0.6 cm × 0.07 cm.

The electrodes were tested in 6 M and 10 M KOH solutions (prepared from AR KOH pellets in ion-exchanged water). The following tests were per-

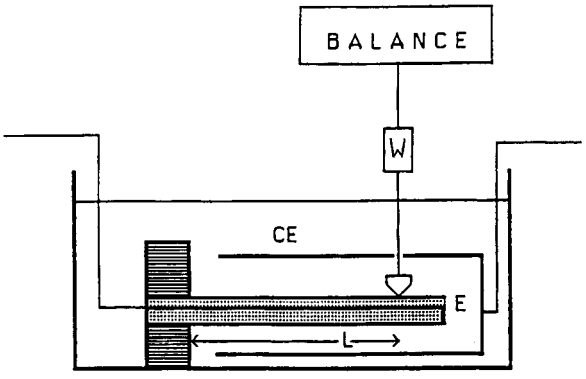

Fig. 2. Cell for electrochemical and mechanical tests.

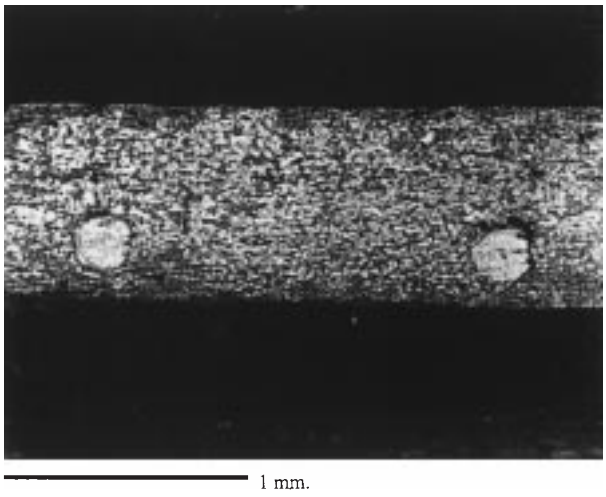

Fig. 3. SEM cross section of an asymmetric NOE (×50).

formed: (a) normal cycling at 1 *C* rate, (5–10% overcharge); (b) shallow discharge, 1 *C* rate, (discharge to 20–50% DOD); and (c) sustained overcharge, 1 *C* rate (2–5 h overcharge).

A typical record of voltage, force and current against time during the discharge–charge cycle is shown in Fig. 4. A good representation of the internal stress changes during cycling is given by the plot of force against capacity. When performing a cycle with a generic system of variables, the common starting point is when the variable under study is at the minimum value. For the NOE, the starting point is the normally charged electrode (not overcharged), when the the active mass is in the highest density state (β-NiOOH) and the lowest stresses on the structure are expected. In the plot, the charge delivered is positive and the charge accepted negative. Figure 4 is replotted in Fig. 5 where (a) relates to the force and (b) to the potential against capacity; the arrows indicate the sequence of the experimental points with respect to time, so arrows towards the right indicate discharge and those towards the left show recharge. All the following plots were drawn in the same way.

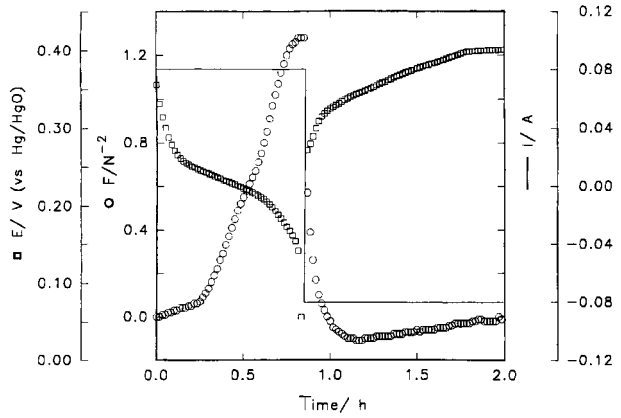

Fig. 4. Typical record of force (*F*), voltage (*E*) and current (*I*) against time, during a discharge–charge cycle.

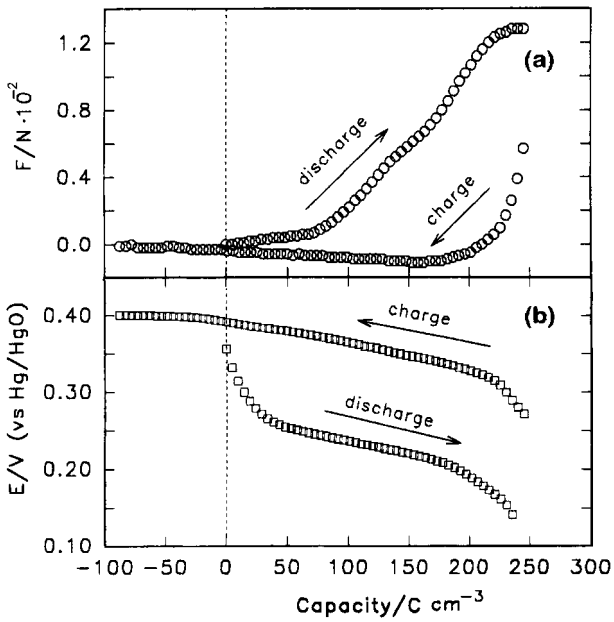

Fig. 5. Plot of data of Fig. 4 against capacity.

3. Results and discussion

3.1. *Electrochemical tests*

Results for the three electrodes (A, B and C) under various conditions, are shown in the lower parts of the plots in Figs 6–10. The discharge curves after a

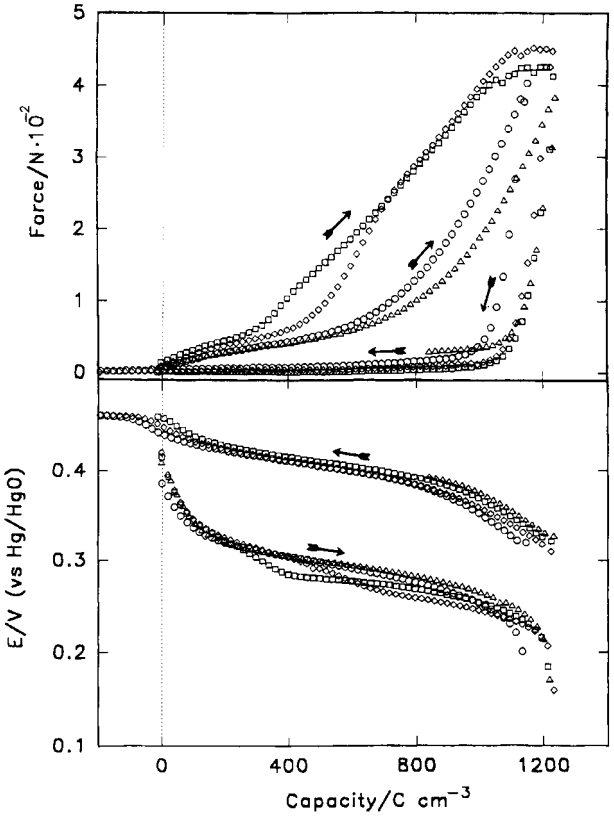

Fig. 6. Force and potential against capacity. Electrode (type A): 6 M KOH at 20 °C. Key: (○) cycle 135, regular charge; (□) cycle 114, 19 shallow cycles, discharge 30% DOD; (◇) cycle 132, 11 shallow cycles, discharge 36% DOD; (△) cycle 116, overcharge 1 *C*, 2 h.

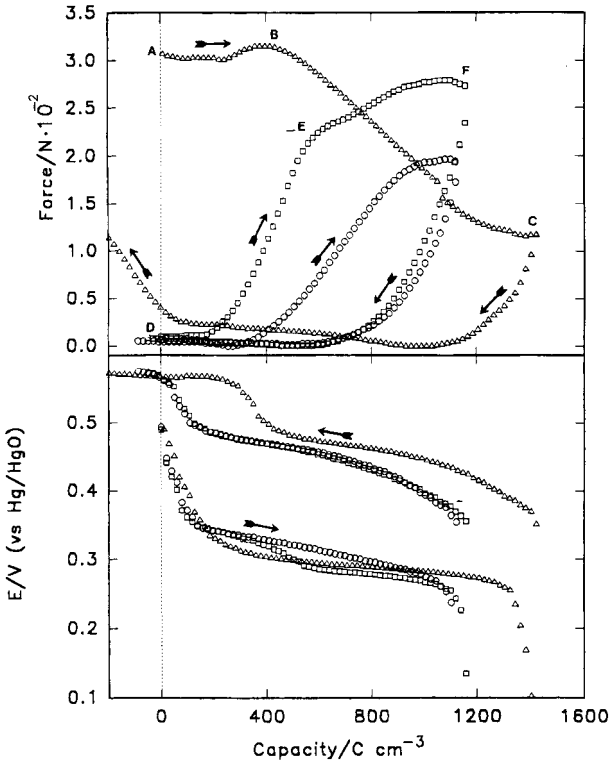

Fig. 7. Force and potential against capacity. Electrode (type B): 6 M KOH at 20 °C. Key: (○) cycle 118, regular charge; (□) cycle 114, 48 shallow cycles, discharge 50% DOD; (△) cycle 122, overcharge 1 *C*, 2 h.

regular charge show the normal sigmoid pattern for all three types of electrode. The discharges after shallow cycles show the voltage step, known as the 'memory effect'. This step occurs at the same depth of discharge (DOD) as the repeated shallow discharges and its voltage/capacity gradient is lower than in the first step and normal discharge. This suggests some degree of phase transition associated with the electrochemical reduction. It has been shown by Kozawa and Powers [13] that the E/C gradient tends to zero when a phase transition occurs in an electrochemical process. According to Oshitani *et al.* [14] during the first step the reduction β-NiOOH $\rightarrow$ β-Ni(OH)$_2$ occurs, without phase transition, and in the second, at lower potential, the reduction γ-NiOOH $\rightarrow$ α-Ni(OH)$_2$, with phase transition, occurs.

The discharge curves after an overcharge in 6 M KOH (2 h at the *C* rate) differentiate the electrodes: type B shows a voltage depression and a noticeable increase in capacity (Fig. 7), whereas types A and C do not show differences with respect to the curves after a regular charge (Figs 6 and 8).

At higher KOH concentrations (10 M) all the electrodes show a two-step discharge curve after shallow cycling, and type C shows the voltage depression after overcharge (Fig. 9), thus confirming that the KOH concentration assists the γ-phase formation [5, 15].

Concerning the influence of the cobalt content on the electrochemical behaviour under experimental conditions, electrode B (Co 4.3%) shows the highest

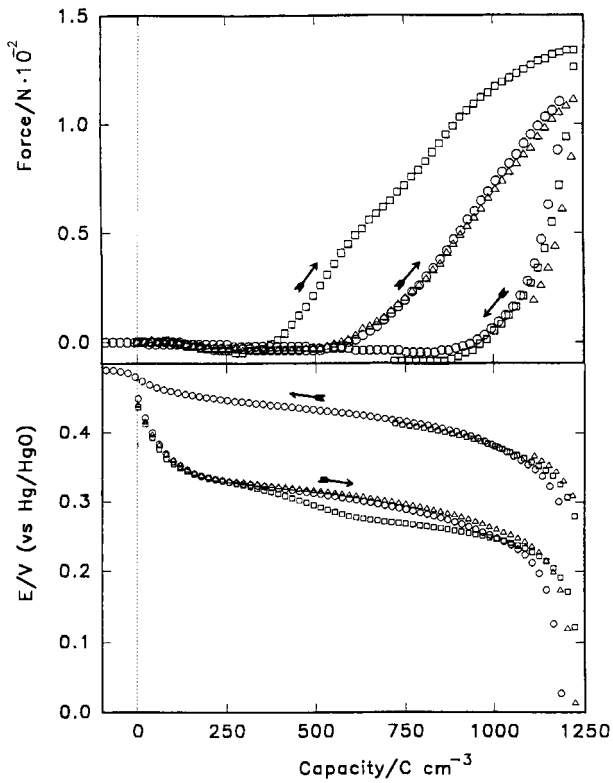

Fig. 8. Force and potential against capacity. Electrode (type C): 6 M KOH at 20 °C. (○) cycle 190, regular charge; (□) cycle 183, 22 shallow cycles, discharge 50% DOD; (△) cycle 191, overcharge 1 *C*, 2 h.

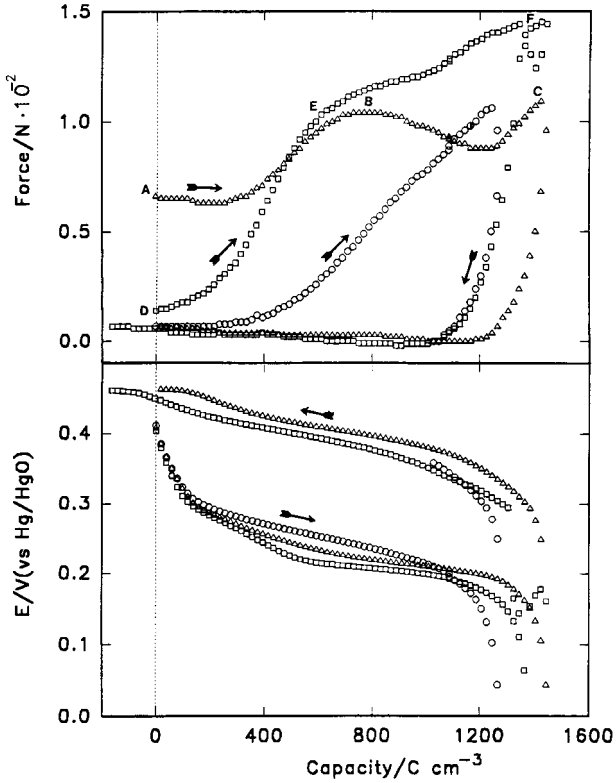

Fig. 9. Force and potential against capacity. Electrode (type C): 10 M KOH at 20 °C. (○) cycle 213, regular charge; (□) cycle 210, 16 shallow cycles, discharge 40% DOD; (△) cycle 212, overcharge 1 *C*, 2 h.

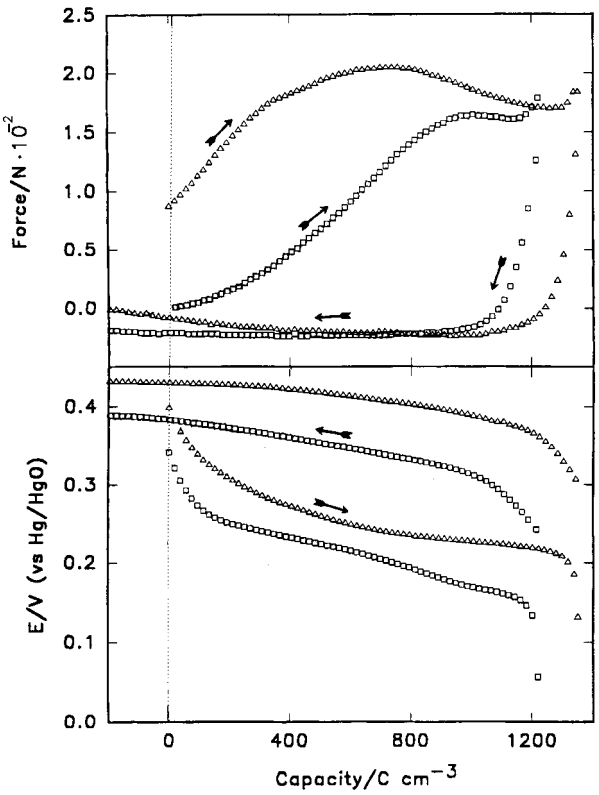

Fig. 10. Effect of temperature on γ-phase formation under overcharge. Electrode (type A): 10 M KOH. Force and potential against capacity. Key: (□) cycle 520 at 20 °C, overcharge 1 *C*, 3.5 h; (△) cycle 558 at 40 °C, overcharge 1 *C*, 3.5 h.

susceptibility to voltage depression after overcharge, and therefore to γ-phase formation, as will be confirmed later by mechanical tests.

3.2. *Mechanical measurements*

The plots of force against capacity, related to the electrochemical data discussed in the previous Section, are shown in the upper parts of Figs 6–10. Under regular cycling the plots show a characteristic pattern: a more or less regular increase in the force as the discharge proceeds and a sudden fall as the new charge begins.

Considering the data in 6 M KOH at 20 °C (Figs 6–8) and after regular charge, electrode type A (Fig. 6) shows a force increase after the early stages of the discharge, then a further growth, and at the beginning of the charge, falls rapidly to zero after about 10% of recharging. After shallow cycling the force begins to increase at the same DOD of the shallow cycle, in any case at lower DOD than after regular cycling.

In the case of a type C electrode (Fig. 8), the increase in force during the discharge after regular charge, begins at about 50% DOD and tends to be linear. After shallow discharge, the force increase begins at the DOD of partial discharge. There is no substantial difference in the behaviour after overcharge and after regular charge. The decrease in the force at the current inversion is fast, but not so much as for the A-type electrode. It is completed at about 20% of recharging.

Electrode type B (Fig. 7) exhibits, in the discharge after regular charge, a stage of linear increase in force and a trend to saturation near the end of the discharge. This pattern is enhanced in the discharge after shallow cycles. The discharge after overcharge is characteristic, since the starting point is in a condition of high stress, as during the overcharge the force increases progressively reaching values higher than the normal value at 100% DOD, relative to β-$Ni(OH)_2$. In Fig. 7 the discharge starts with a high force value (point A); this remains about constant for some 30% DOD (point B), then it decreases linearly to point C, relative to the complete discharge. It is also evident that the force increases at the beginning of the subsequent overcharge (bottom left of the plot).

These stress changes can be related to the molar volumes of the nickel oxyhydroxides participating in the electrochemical process. In Table 1 the densities and the crystallographic parameters of the relevant compounds are tabulated. These data, related to the Bode cycle [19] reported in Fig. 11 help to explain the mechanical behaviour observed, although they are referred to dry conditions.

Regarding the mechanical state, the charged electrode can be unstressed ($F = 0$) or stressed ($F > 0$). The active mass of charged unstressed NOE is the β-NiOOH phase, the densest form; in the charged stressed NOE some γ-NiOOH must be present, this form being less dense by 23%. The presence of γ-phase in overcharged NOE has been proved experimentally [6, 15]. It can thus be deduced that the increase in stress during overcharge of NOE is associated to with the γ-phase formation.

We have F > O, with electrode B, in solution 6 M KOH at 20 °C. (Fig. 7), with electrode C, in 10 M, 20 °C (Fig. 9) and electrode type A in 10 M solution at 40 °C (Fig. 10). These results confirm that the rate of γ-phase formation is higher the higher are the KOH concentration and the temperature. The susceptibility to γ-phase formation during overcharge is in the order type B > type C > type A. This suggest that the cobalt content alone is not a conditioning factor; moreover, the structure and distribution of the active mass, deriving from the impregnation method, can play a role. Electrode type A was produced by chemical impregnation, so it is less porous than types B and C which were electrochemically impregnated.

Table 1. Crystallographic parameters of the hexagonal unit cell and densities of nickel oxyhydroxides

Nickel oxyhyroxide	*a*/cm^{-8} *[16, 17]*	*c*/cm^{-8} *[16, 17]*	*Density*/g cm^{-3} *[18]*
α-$Ni(OH)_2$	3.13	8–9	2.82
β-$Ni(OH)_2$	3.13	4.6	3.97
β-NiOOH	2.82	4.7	4.68
γ-NiOOH	2.82	7.2	3.79

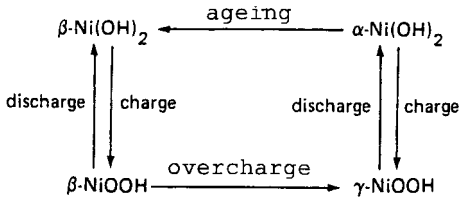

Fig. 11. Bode cycle.

The low porosity of type A hinders the diffusion of K^+ ions taken up by the active mass during the $\beta \rightarrow \gamma$ transition.

The discharge of an overcharged electrode involves the γ-NiOOH $\rightarrow$ α-Ni(OH)$_2$ electrochemical reduction, with expansion, followed by the transition α-Ni(OH)$_2$ $\rightarrow$ β-Ni(OH)$_2$ with contraction. As a consequence, a maximum in the force against capacity plots might be expected, depending on the rate of phase transition α-Ni(OH)$_2$ $\rightarrow$ β-Ni(OH)$_2$.

If the rate of transition is high the process becomes γ-NiOOH $\rightarrow$ β-Ni(OH)$_2$ with a contraction and a negative gradient in the force against capacity plot. Moreover, the distribution of the phases in the body of the electrode cannot be neglected. It has been found, by Thaller and Zimmermann [5], that the molar fraction of γ-phase in a charged nickel electrode after 72 h standing ranges from unity to 0.6 in the first ten micrometres from the current collector. This type of uneven distribution is particularly enhanced in shallow cycles, when the fraction of the active mass in proximity to the current collector is held in the charged state, then suitable for transition to γ-NiOOH, while the rest of the active mass is cycled in the β-phase. Finally, during each discharge of the half partial cycles, K^+ ions migrates toward the inner zone of the electrode and are then ready to enter the structure of the γ-phase during the following charge half-cycle. This model explains how, in general, it is easier to obtain the γ-phase by shallow cycling than by overcharging.

The force against capacity plots after shallow cycles are characterized by an increase of force, thus by a stress on the supporting structure at a lesser DOD than after a regular charge. This feature was common to all the electrodes in all the experimental conditions examined. The results agree with the model suggested, involving transformation to γ-phase of the uncycled fraction of the active mass. This fraction progressively expands, so that less and less void remains for the expansion β-NiOOH $\rightarrow$ β-Ni(OH)$_2$, thus the stress increases earlier. When the reduction of the inner γ-phase begins, the voltage step and the change in slope occur, due to the γ-NiOOH $\rightarrow$ α-Ni(OH)$_2$ reduction, followed by the transition α-Ni(OH)$_2$ $\rightarrow$ β-Ni(OH)$_2$, with volume contraction and stress relief (point E in Figs 7 and 9).

The anticipated increase in stress, due to shallow cycles, must be taken into account when planning the use of a battery, for example, in an automatic guided vehicle (AGV). The plots in Fig. 8 show that in regular cycling a type C electrode can be discharged to 50% DOD without any stress on the structure, but after 16 shallow cycles at 40% DOD it suffers about half the 100% DOD stress, with a potential step 30 mV lower.

The effect of the temperature on γ-phase formation under overcharge is shown in Fig. 10 for a type A electrode. The change of active mass into γ-phase can be achieved by overcharging the electrode 2 h at the *C* rate in 10 M KOH and 40 °C. No phase change is obtained by overcharging at lower temperature and concentration.

4. Conclusions

Shallow discharges, overcharges and normal cycling were carried out on NOEs in KOH at different concentrations and temperatures. An experimental correlation has been found between electrochemical and mechanical behaviour of NOEs subjected to cycling regimes causing the so-called 'memory effect'. The correlation is based on the generally accepted data on molar volumes of the structural phases of nickel oxyhydroxides (i.e., α-Ni(OH)$_2$, β-Ni(OH)$_2$, β-NiOOH and γ-NiOOH) involved in the electrochemical cycling.

The significant results are as follows:

(i) NOE gives a contribution to the memory effect of nickel–cadmium batteries.

(ii) The voltage step in the discharge after shallow cycles occurs at the same DOD of the shallow cycles, and its value is higher the higher the number of these cycles. The mechanical behaviour after shallow cycles shows an increase in stress at lower DOD than in regular cycles, so that shallow cycles at medium DOD can be dangerous for the structure.

(iii) Overcharge causes stress, related to the expansion in the transition β-NiOOH $\rightarrow$ γ-NiOOH. The discharge of the stressed electrodes can produce further stress, due to the γ-NiOOH $\rightarrow$ α-Ni(OH)$_2$ transition, then the stress is reduced if the α-Ni(OH)$_2$ $\rightarrow$ β-Ni(OH)$_2$ transition is fast.

(iv) The susceptibility of tested electrodes to γ-phase formation during overcharge is in the order: type B > type C > type A; this increases by increasing the KOH concentration, temperature, and time.

(v) Shallow cycling is, in general, more effective in forming the γ-phase than overcharging. Shallow-cycled NOEs are never stressed in the charged state, suggesting that the γ-phase is localized in the proximity of the current collector.

(vi) The dynamic method used for studying *in situ* the mechanical behaviour of asymmetric electrodes under cycling gives useful information for modelling the charge and discharge of NOEs.

Acknowledgements

The financial support of MURST, Ministero per L'Università e la Ricerca Scientifica, Roma, is

gratefully aknowledged. The type A test electrode was supplied by Eagle Picher Industries, Colorado Springs, CO, for which we thank G. Brown. Types B and C test electrodes were supplied by the Office of Research and Development of the US Central Intelligence Agency, for which we thank J. Stockel.

References

[1] 'Nickel–Cadmium Battery Application Engineering Handbook', General Electric Company, Publication GET-3148A, Gainesville, FA (1975), Section 6–9.
[2] T. R. Crompton, 'Battery Reference Book' (Butterworts, London, 1990), Section 19–12.
[3] R. N. Thomas, *in* 'Modern Battery Technology', edited by C. D. S. Tuck (Ellis Horwood, New York, 1991), p. 276.
[4] R. Barnard, G. T. Crickmore, J. A. Lee and F. L. Tye, 'Power Sources 6', edited by D. H. Collins (Academic Press, London, 1977), p. 161.
[5] L. H. Thaller and A. H. Zimmerman, *J. Power Sources* **63** (1996) 53.
[6] Y. Sato, K. Ito, T. Arakawa and K. Kobayakawa, *J. Electrochem. Soc.* **143** (1996) L225.
[7] G. Davolio, E. Soragni, A. Da Pieve and S. Forti, Proceedings of the 33rd International Power Sources Symposium, The Electrochemical Society, Pennington, NJ (1988), p. 520.
[8] G. Davolio, E. Soragni, A. Da Pieve and L. Barozzi, ECS Fall Meeting, Phoenix, AZ, 13–17 Oct. (1991). Extended Abstracts, Vol. 91–2 The Electrochemical Society, Pennington, NJ (1991), Abstract 13 p. 19.
[9] G.Weidmann, P. Lewis and N. Reid (Eds), 'Structural Materials' (Butterworths, London, 1990), p. 332.
[10] G. Davolio, Mechanical Properties of Electrodes, *in* 'Nickel–Cadmium Battery Handbook', edited by S. Gross (J. Wiley & Sons, New York, in press.
[11] D. H. Fritts, *J. Power Sources* **12** (1984) 267.
[12] R. P. Feyman, R. B. Leighton and M. Sands, 'Lectures on Physics'; Vol.2 (Addison-Wesley, Reading, MA, 1966), Section 18–9.
[13] A. Kozawa and R. A. Powers, *J. Electrochem. Soc.* **113** (1966) 870.
[14] M. Oshitani, T. Takayama, K. Takashima and S. Tsuji, *J. Appl. Electrochem.* **16** (1986) 403.
[15] R. Barnard, C. F Randell and F. L. Tye *ibid.* **10** (1980) 109.
[16] A. Delhaye-Vidal and M. Figlarz, *ibid.* **17** (1987) 589.
[17] C. Faure, C. Delmas and M. Fouassier, *J. Power Sources* **35** (1991) 279.
[18] H. Bode, K. Dehemelt and J. Witte, Z. Anorg. Allg. Chem. **366** (1969) 1.
[19] H. Bode, K. Dehemelt and J. Witte, *Electrochim. Acta* **11** (1966) 1079.